RSC Advances

COMMUNICATION

View Article Online
View Journal | View Issue

Cite this: *RSC Adv.*, 2014, **4**, 33160

Received 15th May 2014
Accepted 7th July 2014

DOI: 10.1039/c4ra04590d

www.rsc.org/advances

Nitroaldol condensation catalyzed by topologically modulable cooperative acid–base chitosan–TiO_2 hybrid materials†

Abdelhfid Aqil,*[a] Abdelkrim El Kadib,*[b] Mohamed Aqil,[ac] Mosto Bousmina,[bd] Abderrahman Elidrissi,[c] Christophe Detrembleur[a] and Christine Jérôme[a]

Chitosan–TiO_2 shaped as macroporous aerogels, lamellar cryogels or electrospun films act synergistically as acid–base bifunctional catalysts. Depending on the topology of the material, a marked difference in the selectivity for nitroaldol condensation is observed.

Inspired by the ability of enzymes to tune cooperative interactions in confined environments, sustained efforts have been devoted to design acid–base bifunctional building blocks for applications such as ligand–receptor binding,[1] non-metallic activation,[2] adsorption[3] and catalysis.[4] In contrast to the homogeneous acid–base motifs, for which an abundant literature exists, acid–base synergy in heterogeneous materials is relatively less addressed and there are plenty of opportunities for such materials to be discovered and explored. Very recently, cooperative solid materials, including aluminophosphates,[5] lamellar clay,[6] mesoporous organosilica[7] and metal organic framework,[8] were reported. Attaching acidic and basic species in close vicinity through chemical synthesis is thus possible, but generally it requires complex and time-consuming multi-step synthesis routes. In contrast, conferring acid–base bifunctional character through the entrapment of specific selected nanoparticles in a given basic or acidic chemical medium is an attractive strategy that can be applied for a wide spectrum of cost-effective applications.[9] In this respect, we have recently shown that chitosan, a natural amino-carbohydrate driven from biomass resources, can self-assemble to control the nucleation and growth of titanium-based sol–gel species at "the fibrillar level" affording—after CO_2 supercritical drying—macroporous chitosan–titania (**CS–TiO_2**) hybrid materials.[10,11] The presence of amino groups in the chitosan backbone in close proximity to the nanosized Lewis acidic titanium oxide clusters "$NH_2\cdots$Ti–O–Ti" confers an unusual acid–base cooperative character to these materials, which has been advantageously exploited for fine chemical synthesis (Fig. 1).[10–13]

Among the exciting advantages of chitosan are its ability to afford open framework hydrogels by pH inversion (coagulation of acidic soluble polymer in base bath),[11] and its versatility for providing different macroscopic topologies (microspheres, monoliths, thinner or thicker films and ultra-fine particles).

Moreover, trimodal micro-, meso- and macro-porosity of the resultant polymeric network can also be tuned.[11,14] Chitosan and its blended polymeric versions can also be shaped in the form of nano- and micro-fibrils by electro-spinning and other processes for membrane applications.[15] Furthermore, the replication of inorganic oxide occurring within the entangled porous light-weight aerogels (at the fibrillar level) can be reproduced within the electrospun chitosan-based nanofibers, for which the material is shaped as a membrane (flat surface) rather than porous microspheres (convex surface).

Considering the paucity of literature reports regarding the influence of the macroscopic topology and related textural properties on the cooperative catalytic activity, these materials seem to be an ideal prototypical quest. Herein, we focus on the preparation of three textured chitosan–titania catalysts, featuring similar chemical composition "$NH_2\cdots$Ti–O–Ti" but with different topologies, *i.e.* convex **CS–TiO_2–Aero** or flat

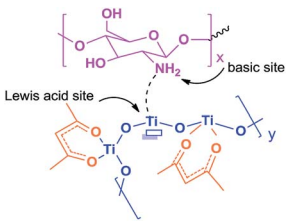

Fig. 1 Illustration of the acid–base cohabitation within the framework of chitosan–titania hybrid materials.

[a]*Center for Education and Research on Macromolecules (CERM), University of Liège, B6a B-4000 Liège, Belgium. E-mail: a.aqil@ulg.ac.be*

[b]*Euro-Mediterranean University of Fez (UEMF), Fès-Shore, Route de Sidi harazem, Fès, Morocco. E-mail: a.elkadib@ueuromed.org*

[c]*University Mohammed Ier, Oujda, BV Mohammed VI B.P. 524, Oujda 60000, Morocco*

[d]*Hassan II Academy of Science and Technology, Morocco*

† Electronic supplementary information (ESI) available: Synthesis and characterizations of precursors and materials. See DOI: 10.1039/c4ra04590d

surfaces **CS–TiO$_2$–F** and outer-sphere surfaces such as open **CS–TiO$_2$–Aero** or lamellar **CS–TiO$_2$–Lyo**, and examine the similarities and the differences in their behaviour during synergistic acid–base heterogeneous catalysis.

The starting microspheres were prepared by solubilizing chitosan in acidic solution (to generate a soluble ammonium polymer), and its subsequent introduction as droplets in 0.1 N NaOH base bath *via* a needle. This induces deprotonation of the ammoniums, which causes the insoluble amines to immediately form an entangled fibrillar hydrogel-shaped as self-standing microspheres (2 wt% of the polymer dispersed in 98 wt% water).[11] After extensive washing until pH ~7, the beads can be exchanged to alcohol, and then to CO_2 for supercritical drying (**CS–Aero**) or can be directly lyophilized (**CS–Lyo**).[16] Although the open framework of the initial hydrogel could be stabilized by supercritical drying (**CS–Aero**), partial collapse of the lyophilized microspheres (**CS–Lyo**) is observed, causing a significant alteration of the fibrillar network to generate a layered lamellar structure. The third material is prepared by electro-spinning chitosan to generate polysaccharide thin films built from nanofibers (**CS–F**).[15] The common thread in these materials is their fibrillar network (Fig. 2: middle), amenable to replicate titanium alkoxide precursors leading to three **CS–TiO$_2$** materials.[16] Although $Ti(OiPr)_4$ coating is found to be hardly controllable, switching to the less reactive $Ti(OiPr)_2(acac)_2$ affords an aggregation-free, finely decorated polysaccharide fibrillar network. SEM analyses of the three **CS–TiO$_2$** have evidenced that the petrification occurs at the fibrillar surface with no phase separation or uncontrolled growth outside of the fibers, and the resultant materials maintain textural properties similar to those of the starting polymer **CS** (Fig. 2: right). To accurately establish the chemical structure of these materials after sol–gel coating, a MAS ^{13}C NMR has been recorded and compared with literature data of nonmodified chitosan.[17] **CS–TiO$_2$** materials exhibit two peaks around 24 and 174 ppm, assignable to the methyl and carbonyl groups of the acetamide moieties. Four peaks attributable to the pyranose ring skeleton have also been shown at 55, 75, 82 and 105 ppm, indicating that no transformation occurred on the polymeric chains (neither fragmentation nor ring opening or disproportionation) as a consequence of titanium alkoxyde mineralisation. Two additional peaks are observed at 118 and 195 ppm, unambiguously assigned to residual acetylacetonate groups bridged to the metal center.[16] This is consistent with the fast hydrolysis–condensation of the alkoxyde groups (compared to the acac fragments) in $Ti(OiPr)_2(acac)_2$, therby forming oxo-clusters in which acetylacetonates are ligated on the surface of the growing hybrid materials.[18] Owing to the presence of titanium clusters, DRUV analysis of **CS–TiO$_2$** shows a broad oxygen → metal charge transfer (CT) absorption band with a maximum at 312 nm, indicative of the incipient oligomerisation of Ti(IV) species.[19]

The presence of titania has been conclusively corroborated by EDX and XPS analyses. EDX was used for Ti mapping, and it revealed the homogeneous distribution of titanium species within the polymeric network, thereby excluding the formation of core–shell-type hybrid materials.[16] XPS was performed in order to elucidate the nature of the titania species in these composite materials. Indeed, an expected signal has been observed at 458.3 eV, typical of titanium oligomeric clusters.[20] Insight on the chemical interplay between the glucosamine units of the chitosan backbone and titanium dioxide centers has been gained by means of XPS analysis. The observation of two peaks at 399 and 401 eV indicates the presence of two nitrogen species. The former at 399 eV is characteristic of free amine (similar to those observed in native chitosan), while the latter at 401 eV is typical of quaternized, lower metal coordinated NH_2 → Ti.[16] The amount of the loaded titanium oxide clusters estimated by thermogravimetric analysis (TGA) ranges from 15 to 23 wt%. Some intrinsic characteristics of these three materials are gathered in Table 1.

To verify the synergistic acid–base cooperation of **CS–TiO$_2$** hybrid materials, the nitroaldol condensation, commonly referred to as the Henry reaction (Scheme 1) has been selected as a prototype reaction (extensively studied reaction). Indeed, Katz *et al.* previously correlated the type of products (nitrostyrene **I** or nitroaldol **II**) to the dielectric-outer spheres of the amine catalyst tethered on the silica surface.[21] Asefa nicely tuned the selectivity in the nitroaldol condensation by supporting primary, secondary or tertiary amines on the silica

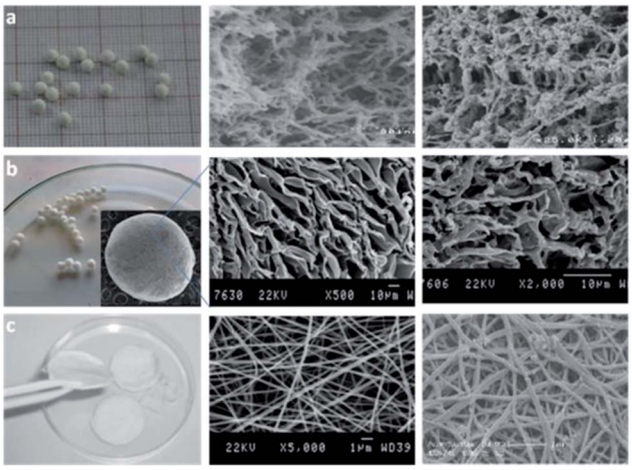

Fig. 2 Left. Digital photos of the prepared materials. (a) CS–Aero. (b) CS–Lyo (inset: SEM of the croygel bead) and (c) CS–F. Middle: SEM photos showing the fibrillar network of the polymer. Right: SEM photos of the respective materials after sol–gel coating (CS–TiO$_2$). The fibrillar network is preserved.

Table 1 Textural properties of CS–TiO$_2$

Material	S_{BET} [a]	% TiO_2	S_{BET} [b]	Fiber diameter
CS–TiO$_2$–Aero	120	23	480	35 nm
CS–TiO$_2$–Lyo	71	15	120	1.05 µm
CS–TiO$_2$–F	—	20	—	230 nm

[a] S_{BET} (m^2 g^{-1}) from nitrogen sorption analysis before titania mineralization. [b] S_{BET} (m^2 g^{-1}) from nitrogen sorption analysis after titania mineralization.

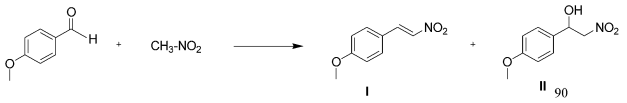

Scheme 1 Henry reaction (aldol condensation) yielding nitroalkene I or nitroalcohol II depending on the outer-sphere polarity of the surrounding catalyst.

surface.[22] Mechanistically speaking, this reaction is shown to proceed *via* ion-pair mechanism (formation of nitroaldol **II**) or imine intermediates (formation of nitrostyrene **I**).

To ascertain first whether the three chitosan forms (**CS–Aero**, **CS–Lyo** and **CS–F**) are valuable for catalysis, these amines crowded in various environments were subjected to nitromethane for a *para*-methoxybenzaldehyde condensation and compared to homogeneous NEt_3 and $EtNH_2$. Comparison of the catalytic activity of **CS–Aero**, **CS–Lyo** and **CS–F** reveals that **CS–Aero** is the most active catalyst, performing a satisfactory conversion of 68% in 24 hours, whereas **CS–Lyo** and **CS–F** provide, after the same period of time, only 23% and 27% conversions, respectively (Fig. 3a). This behaviour is due to the accessibility issue as **CS–Aero** features the highest surface area and the largest macroporous network making more than 75% of its amine groups accessible for catalysis.[11,23] The layered framework in the case of **CS–Lyo** and the densely distributed polymeric fibers in **CS–F** cause a great number of amine groups to be sequestered within the packed network and consequently devoided from any catalytic activity. Homogeneous $EtNH_2$ accomplishes an outstanding 90% conversion after only 5 hours, illustrating thus the higher reactivity of homogeneous species even over the highly porous **CS–Aero** (Fig. 3a).

Having validated that the openness of the framework affects the reaction kinetics, the question was whether or not these textured materials could preserve their synergistic acid–base character or if the evolution of the gelling microstructure to lamellar structure in **CS–Lyo** and the flatness of the surface in **CS–F** would suppress these properties. To this end, the behaviour of **CS–TiO_2–Aero**, **CS–TiO_2–Lyo** and **CS–TiO_2–F** was investigated in the Henry condensation.

The comparison of hybrids **CS–TiO_2** with the starting native chitosan **CS** reveals that the presence of titanium clusters significantly boosts the catalytic activity, which enables quantitative conversion of the reactants (Fig. 3b).

When comparing the three catalysts, the same trend (as for native chitosan) is observed with **CS–TiO_2–Aero** being the most active one (98% after 3 h), followed by **CS–TiO_2–Lyo** (99% in 24 h), while the flattened surface **CS–TiO_2–F** needed 48 hours to accomplish quantitative conversion. This unambiguously demonstrates that, independent of the porosity type, **CS–TiO_2** materials preserve their acid–base synergistic cooperation in catalysis. However, the state of the framework (opened, lamellar or flattened) plays a key role in accelerating the conversion kinetics, as expected.

Taking a closer look at the forming products (aldol *versus* alkene products), a dramatic switch in the reaction selectivity is observed (Fig. 4). Although **CS–TiO_2–Aero** affords almost selectively the nitrostyrene product (ratio of alkene : alcohol = 95 : 5), it is totally inverted in the case of **CS–TiO_2–Lyo** (ratio of alkene : alcohol = 9 : 91) and for **CS–TiO_2–F** (ratio of alkene : alcohol = 7 : 93). The predominance of nitrostyrene over nitroalcohol in the case of **CS–TiO_2–Aero** indicates that the condensation occurs herein by an imine formation mechanism reminiscent of that occurring with the hydrophilic silica tethered aminopropyl catalyst.[21] In this latter case, the surface silanols act in synergy with tethered amine groups as Si–OH are involved in the formation of imine and iminium (both of them are intermediates in nitrostyrene formation).[21] Hydrophobic silica in which Si–OH are end-capped to provide $Si–OSiMe_3$ does not allow this synergy and under these conditions, the reaction proceeds *via* ion pair mechanism to preferentially produce the nitroaldol product.[21] Similarly herein, **CS–TiO_2–Aero** is distinguished from its lyophilized **CS–TiO_2–Lyo** or flattened-surface **CS–TiO_2–F** version by the abundance of Bronsted OH groups and accessible Lewis acid titanium centers, both of them can catalyze, similar to silanol, the imine and iminium formation. This explanation seems to be reasonable as the fibrillar network of the polymeric chains appears more accessible in the aerogels as a result of the three-dimensional network, drawn one-each-other in the layered, partially collapsed lyophilized cryogels and well-packed in the case of the flattened films. In the two latter cases (layered or packed), this probably leads to: (i) the confinement of the replicated species in a constrained space, making the simultaneous accessibility of the two reactants to the collaborative active sites environment more difficult (kinetic effect), and (ii) the consumption of the hydroxylic groups belonging to the organic polymer and those resulting from the

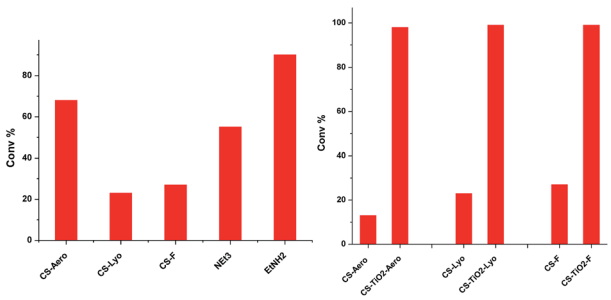

Fig. 3 (a) Left: conv. (%) obtained using different aminated catalysts. (b) Right: comparison of the conv. (%) using mono-(CS) *versus* bifunctional (CS–TiO_2) catalysts.

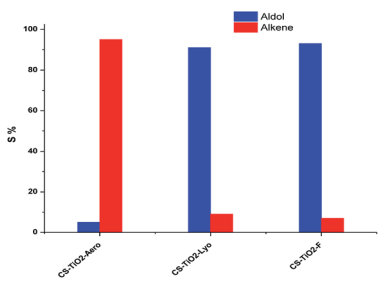

Fig. 4 Aldol-to-alkene ratio obtained with the three CS–TiO_2.

incomplete condensation of titania species (Ti–OH), thereby affecting the outsphere polarity (selectivity effect).

The recyclability of **CS–TiO_2** materials has been assessed and regardless of the topology of the material, the three mineralized catalysts can be recovered and reused several times (up to four times for **CS–TiO_2–Aero**) without any decrease of their catalytic activity. In contrast, a fast decay of the native chitosan is observed within the first two runs, probably because of its limited thermal and chemical stability.

To sum up, the outersphere environment has been hitherto tailored by means of chemical modification to provide tethered catalyst grown in hydrophilic or hydrophobic medium. Quite recently, supramolecular chemistry based on foldamers[24] and micellar systems[25] have been proven effective for shielding active sites in a confined medium. Herein, the versatility in processing the starting polymer and the control over drying the sol–gel modified chitosan hydrogels enable access to various multi-functional enzyme-like catalysts. This textural engineering has been the driving force to invert the classical selectivity of primary amines for nitroaldol condensation.

Acknowledgements

The authors are grateful to the 'Politique Scientifique Fédérale' for financial support in the framework of the Interuniversity Attraction Poles Programme (IAP VII-05): Functional Supramolecular Systems (FS2), to the Region wallonne (DG06) for support in the frame of GoCell project (grant nos 516025 and 616262) and to the Euro-Mediterranean University for financial support. The authors are thankful to Professor Albert Demonceau (University of Liège) for helpful assistance in GC analysis.

Notes and references

1 M. W. Pantoliano, R. A. Horlick, B. A. Springer, D. E. Van Dyk, T. Tobery, D. R. Wetmore, J. D. Lear, A. T. Nahapetian, J. D. Bradley and W. P. Sisk, *Biochemistry*, 1994, **33**, 10229–10248.
2 D. W. Stephan and G. Erker, *Angew. Chem., Int. Ed.*, 2010, **49**, 46–76.
3 N. A. Brunelli, S. A. Didas, K. Venkatasubbaiah and C. W. Jones, *J. Am. Chem. Soc.*, 2012, **134**, 13950–13953.
4 J. M. Notenstein and A. Katz, *Chem.–Eur. J.*, 2006, **12**, 3954.
5 M. J. Climent, A. Corma, V. Fornés, R. Guil-Lopez and S. Iborra, *Adv. Synth. Catal.*, 2002, **344**, 1090–1096.
6 K. Motokura, N. Fujita, K. Mori, T. Mizugaki, K. Ebitani and K. Kaneda, *J. Am. Chem. Soc.*, 2005, **127**, 9674–9675.
7 For review, see: (*a*) E. L. Margelefsky, R. K. Zeidan and M. E. Davis, *Chem. Soc. Rev.*, 2008, **37**, 1118–1126; (*b*) U. Diaz, D. Brunel and A. Corma, *Chem. Soc. Rev.*, 2013, **42**, 4083–4097; (*c*) S. Shylesh and W. R. Thiel, *ChemCatChem*, 2011, **3**, 278–287; (*d*) M. Tada, K. Motokura and Y. Iwasawa, *Top. Catal.*, 2008, **48**, 32–40.
8 F. Vermoortele, R. Ameloot, A. Vimont, C. Serrec and D. De Vos, *Chem. Commun.*, 2011, **47**, 1521–1523.
9 See for instance: (*a*) B. Voit, *Angew. Chem., Int. Ed.*, 2006, **45**, 4238–4240; (*b*) B. Helms, S. J. Guillaudeu, Y. Xie, M. McMurdo, C. J. Hawker and J. M. Frechet, *Angew. Chem., Int. Ed.*, 2005, **44**, 6384–6387; (*c*) F. Gelman, J. Blum and D. Avnir, *Angew. Chem., Int. Ed.*, 2001, **40**, 3647–3649.
10 A. El Kadib, K. Molvinger, C. Guimon, F. Quignard and D. Brunel, *Chem. Mater.*, 2008, **20**, 2198.
11 A. El Kadib and M. Bousmina, *Chem.–Eur. J.*, 2012, **18**, 8264–8277.
12 A. El Kadib, K. Molvinger, M. Bousmina and D. Brunel, *Org. Lett.*, 2010, **12**, 948.
13 A. El Kadib, K. Molvinger, M. Bousmina and D. Brunel, *J. Catal.*, 2010, **273**, 147.
14 A. El Kadib, M. Bousmina and D. Brunel, *J. Nanosci. Nanotechnol.*, 2014, **14**, 308–331.
15 K. Ziani, C. Henrist, C. Jerome, A. Aqil, J. I. Maté and R. Cloots, *Carbohydr. Polym.*, 2011, **83**, 470–476.
16 See ESI† for details.
17 M. Rinaud, *Prog. Polym. Sci.*, 2006, **31**, 603–632.
18 C. Sanchez, J. Livage, M. Henry and F. Babonneau, *J. Non-Cryst. Solids*, 1988, **100**, 65–76.
19 L. Marchese, E. Gianotti, V. Dellarocca, T. Maschmeyer, F. Rey, S. Colluccia and J. M. Thomas, *Phys. Chem. Chem. Phys.*, 1999, **1**, 585–592.
20 C. D. Wagner, W. M. Riggs, L. E. Davis, J. F. Moulder and G. E. Muilenberg, *Handbook of X-ray Photoelectron Spectroscopy*, Perkin-Elmer Corp., Eden Prairie, MN, 1979, p. 68.
21 D. Bass, A. Solovyov, A. J. Pascall and A. Katz, *J. Am. Chem. Soc.*, 2006, **128**, 3737.
22 A. Anan, R. Vathyam, K. K. Sharma and T. Asefa, *Catal. Lett.*, 2008, **126**, 142.
23 R. Valentin, K. Molvinger, F. Quignard and D. Brunel, *New J. Chem.*, 2003, **27**, 1690.
24 E. Huerta, P. J. M. Stals, E. W. Meijer and A. R. A. Palmans, *Angew. Chem., Int. Ed.*, 2013, **52**, 2906.
25 P. Cotanda, A. Lu, J. P. Patterson, N. Petzetakis and R. K. O'Reilly, *Macromolecules*, 2012, **45**, 2377–2384.